

# Secular variation in carbon isotope ratios from Upper Proterozoic successions of Svalbard and East Greenland

A. H. Knoll\*, J. M. Hayes†, A. J. Kaufman†, K. Swett‡ & I. B. Lambert§

\* Department of Organismic and Evolutionary Biology, Harvard University, Cambridge, Massachusetts 02138, USA

† Biogeochemical Laboratories, Department of Chemistry and Geology, Indiana University, Bloomington, Indiana 47405-5101, USA

‡ Department of Geology, University of Iowa, Iowa City, Iowa 52242, USA

§ Baas Beeking Geobiological Laboratory, PO Box 378, Canberra ACT 2601, Australia

*Analyses of stratigraphically continuous suites of samples from Upper Proterozoic sedimentary successions of East Greenland, Spitsbergen and Nordaustlandet (Svalbard) provide an approximation to the secular variation in carbon isotope ratios during a geologically and biologically important period of change from around 900 million years ago to the beginning of the Cambrian period. Late Riphean carbonates and organic material show a stratigraphically useful pattern of enrichment in  $^{13}\text{C}$  relative to Phanerozoic or earlier Proterozoic samples. Isotopic compositions of isolated samples from other localities are consistent with a worldwide extended interval of enhanced organic burial and consequent net survival of oxidized material, probably  $\text{O}_2$ , just before the initial radiation of metazoans.*

SECULAR variations in the carbon isotopic composition of sedimentary carbonates and organic materials have been determined with reasonable temporal precision for most of the Phanerozoic eon, and these data have assumed a significant role in discussion of Phanerozoic environmental history<sup>1-4</sup>. Analyses of Precambrian samples show that on a gross scale the earlier record of carbon isotopic variation is not dissimilar to that of the past 570 Myr (ref. 5); however, insufficient sampling density and a lack of stratigraphic control have hindered attempts to continue the curve representing of carbon isotopic abundances in marine carbonates backward into the Proterozoic.

We report here the results of carbon isotopic analyses of stratigraphically continuous suites of samples collected from Upper Proterozoic sedimentary successions in Nordaustlandet (Svalbard), northeastern Spitsbergen and central East Greenland. Stratigraphic position, palaeoenvironmental setting and petrography have been determined for each sample, and a degree of biostratigraphic control is provided by acritarch assemblages that occur in all three sequences. The sections, which represent widely separated localities within a single sedimentary basin, show smoothly covariant carbon isotope records for both carbonate and organic carbon. Here we consider three questions bearing on the interpretation and significance of these isotopic variations:

(1) Are they primary (that is, reflective of changes in the isotopic composition of carbon available for biosynthesis of organic matter)?

(2) Are they of global extent (representative of changes in the isotopic composition of oxidized carbon in the world ocean)?

(3) Do they reflect changes in the Earth's surface environment, especially changes in  $\text{O}_2$  concentration, which may have been important in late Proterozoic biological evolution?

## Geological setting

The close lithostratigraphic similarities between the Upper Proterozoic and Lower Palaeozoic sequences of the East Greenland Caledonides and eastern Svalbard have long been appreciated<sup>6</sup>. The Spitsbergen, Nordaustlandet and East Greenland sections each contain 7,000-8,000 m of unmetamorphosed, predominantly shallow marine sedimentary rocks, comprising two quartz-arenite-carbonate successions separated by an interval of glaciogenic sedimentation<sup>7-14</sup>. Table 1 summarizes the nomenclature of the sampled rock units, and stratigraphic columns are shown in Fig. 1.

Thick sequences of cross-bedded and rippled sandstones with

interbedded rippled, often carbonaceous shales grade upward into carbonates with minor siliciclastic intercalations. The limestone and dolostone successions contain abundant stromatolites, cross-bedded oolites and pisolites, and intraformational conglomerates, all of which indicate intertidal to shallow subtidal marine deposition. The carbonates are overlain abruptly by a diamictite-bearing siliciclastic sequence, which is in turn overlain by a quartz-arenite-carbonate sequence of Cambro-Ordovician age. Microfossil assemblages<sup>15-17</sup> and stromatolites<sup>18</sup> indicate that the earlier siliciclastic and carbonate sequence was deposited ~900-700 Myr ago, during the late Riphean interval, and that the diamictite-bearing sequence is Vendian (670-570 Myr) in age. Hiatuses corresponding in time to the latest Riphean and late Vendian to earliest Cambrian occur at the base and top, respectively, of the diamictite-bearing succession<sup>14</sup>. (In Greenland, the stratigraphic break appears to occur not at the Eleonore Bay Group/Tillite Group boundary, but within Bed 19 of the Eleonore Bay Group.)

Petrographic studies reveal further strong parallels in the histories of the Greenland and Svalbard sequences<sup>19</sup>, and palaeontological analyses show comparable patterns of microfossil distribution<sup>15-17,20,21</sup>. Based on these observations, 16 tie-points have been identified which can be correlated lithostratigraphically with high confidence among sections: these are shown in Fig. 1 (the tie-point at the Precambrian/Cambrian boundary is designated zero, and numbers increase down-section). The close correlations show that the three successions were deposited contiguously along the margin of a single marine basin<sup>22</sup>. The distance separating the most distant of the successions at the time of deposition was at least 650 km, and possibly much greater. The East Greenland-Svalbard basin apparently constituted the western margin of the expanding Iapetus Ocean during the Cambrian, but debate continues as to whether the thick underlying Upper Proterozoic sequence accumulated intracratonically or on an early-formed passive margin<sup>22,23</sup>.

## Chemical and isotopic analyses

Field specimens were cleaned, fragmented, etched and ground<sup>24</sup>. Carbon dioxide was produced from carbonates by treatment with  $\text{H}_3\text{PO}_4$  (density 1.89 g ml<sup>-1</sup>) at 50 °C for 48 h (ref. 25). For determination of the abundance and isotopic composition of organic carbon, sample powders were treated with hot, concentrated HCl in order to remove carbonates, then mixed with CuO and sealed in evacuated quartz tubes for combustion at 850 °C for 2 h. Recovery and purification of  $\text{CO}_2$  formed by combustion

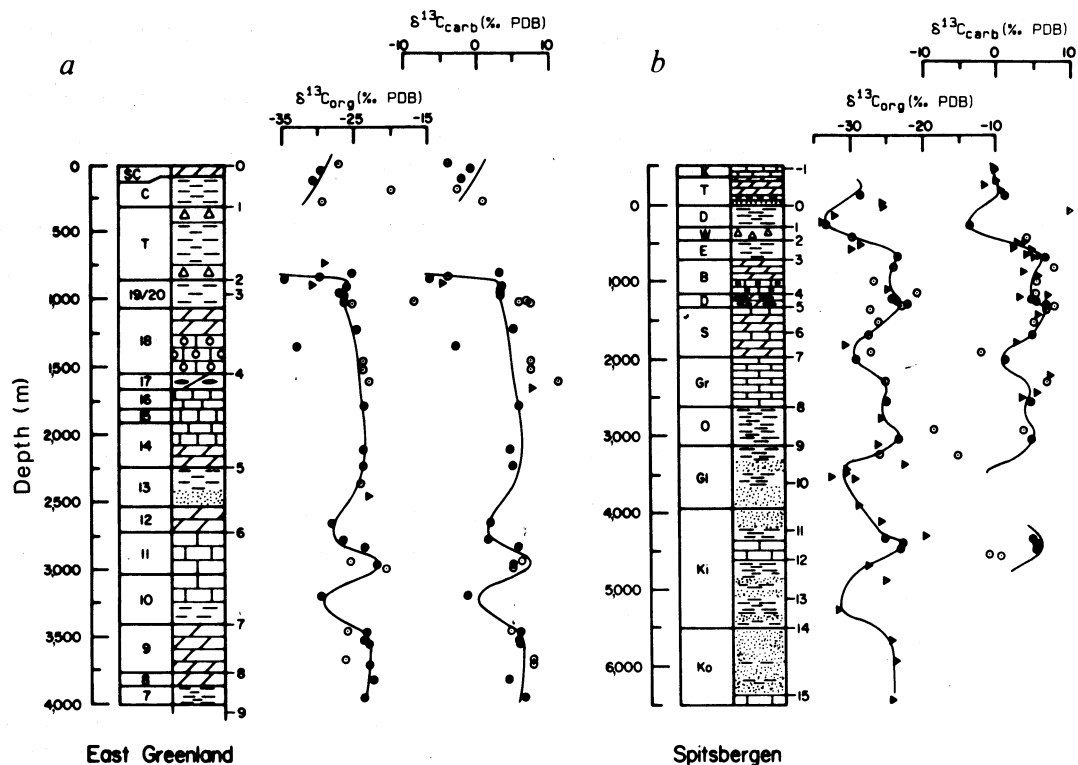
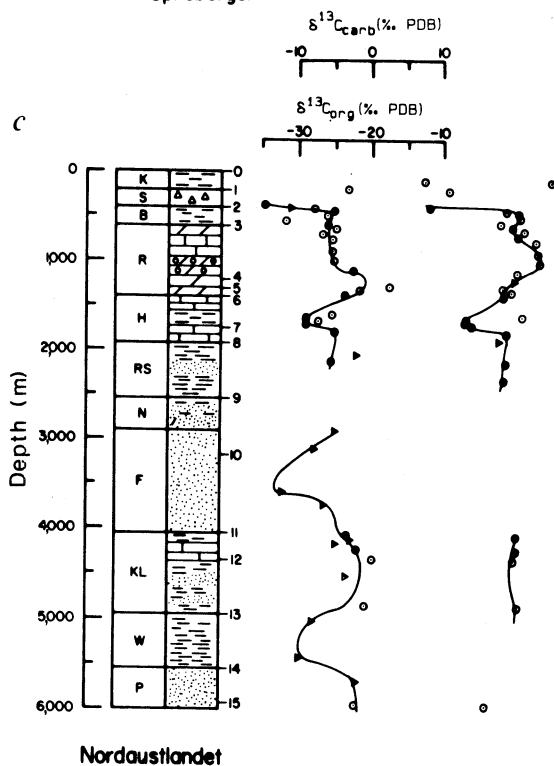


**Fig. 1** Stratigraphic columns and carbon isotopic analyses of organic material and total carbonate from late Proterozoic sediments of East Greenland (a), northeastern Spitsbergen (b) and Nordaustlandet (c). Numbers to the right of the stratigraphic columns indicate tie-points discussed in the text. Full names of formations are given in Table 1. Note that the vertical scales differ. Filled circles represent carbonate-organic pairs with  $26.5 \leq \epsilon \leq 30.5\%$ . Results from other pairs are represented by open and half-filled circles, the latter being used where it is evident that the aberration in  $\epsilon$  is associated with the other point in the pair (for example, an unusually heavy carbonate in a sample yielding  $\epsilon \geq 30.5\%$ ). Open triangles indicate samples for which it was possible to analyse only organic or carbonate carbon (not both). A detailed tabulation of these data (isotopic compositions, lithologies, locations in section) is available from the authors on request.



of organic matter allowed both quantitative and isotopic analysis. This procedure was tested by application to 49 samples previously analysed by accepted techniques<sup>24</sup>, and yielded accurate results for samples similar to those analysed in this work. Isotopic compositions of CO<sub>2</sub> were determined by conventional mass spectrometric techniques<sup>26</sup> and are expressed relative to the PDB standard:  $\delta = [(R_x/R_{PDB}) - 1] \times 10^3$ , where  $R = {}^{13}C/{}^{12}C$  and the subscript  $x$  designates the analyte. For compactness, we employ  $\delta_c$  and  $\delta_o$  to refer to the carbon isotopic compositions of carbonate and organic carbon, respectively.

## Results and discussion

**Isotopic variations.** Figure 1 summarizes the results of the

isotopic analyses: it is evident that the abundance of <sup>13</sup>C varies in both carbonate minerals and organic material. Such variations can be primary (reflecting changes in the isotopic composition of carbonate in the water column beneath which the sediments initially accumulated) or secondary (reflecting bacterial reworking of organic material, precipitation and admixture of new carbonates, or isotopic exchange with species in solution). Consideration of the significance of these isotopic variations requires resolution of primary and secondary effects.

Recognition of truly primary isotopic compositions and perfect elucidation of all secondary variations is difficult in the best of circumstances<sup>27</sup>. However, no secondary processes are known (or are, for that matter, conceivable) which always shift the

isotopic compositions of carbonate and organic carbon in the same direction at the same rate. Instead, secondary processes commonly alter the isotopic composition either of organic carbon<sup>28</sup> or of carbonate carbon<sup>29</sup>, and the magnitudes of the isotopic shifts are controlled by different and unrelated factors. Primary processes (biosynthesis of organic material and formation of carbonate in equilibrium with dissolved CO<sub>2</sub>), on the other hand, tend to maintain a constant isotopic difference between carbonate and organic carbon. Systematic consideration of the isotopic fractionation ( $\epsilon = \delta_c - \delta_o$ ) can therefore assist in the resolution of primary and secondary isotopic variations.

The data include 92 pairs of measurements from which  $\epsilon$  values can be computed; the carbon isotopic compositions of carbonate and organic materials in these samples are compared in Fig. 2. The mode of the distribution of  $\epsilon$  values lies near 28.5% (dashed line in Fig. 2). Many of the carbonate-organic pairs yielding  $\epsilon > 30.5\%$  or  $\epsilon < 26.5\%$  contain  $< 0.2$  mg organic C per g sample or  $< 10\%$  carbonate; because of their low carbon concentrations, the isotopic compositions of these samples are particularly vulnerable to diagenetic alteration. We conclude that samples yielding  $\epsilon = 28.5 \pm 2.0\%$  preserve primary carbon isotopic compositions within a few per mil. We do not contend that isotopic shifts due to diagenesis are absent in these sections, and will return to this point below. We do suggest, however, that measurement of both organic and inorganic carbon isotopic compositions greatly reduces the chance of misinterpretation and allows the recognition of major features in the isotopic records compiled in this work.

**Correlations between sections.** Comparison of variations observed in the different sections suggests that all three record the same set of primary variations. For example, all are depleted in <sup>13</sup>C in the Vendian and show a general pattern of <sup>13</sup>C enrichment during the late Riphean. The lithostratigraphic tie-points already described can be used to plot data from all sections on a single graph, facilitating investigation of isotopic correlations.

In Fig. 3, the ordinate ('stratigraphic position') represents the sequence of tie-points and is thus a scale related to depth. Isotopic compositions of samples collected at stratigraphic levels equivalent to tie-points have been plotted at integer values; others have been placed along the ordinate by linear interpolation between tie-points within each section. The dashed lines are separated by 28.5%, and were derived by overlaying the carbonate and organic carbon isotopic records (offset by 28.5%) and considering the trend of both sets of data. The close parallel between the organic and inorganic records is clearly visible in the upper part of the section. Carbonates are rare in the lower part of the section, but strong evidence for additional isotopic

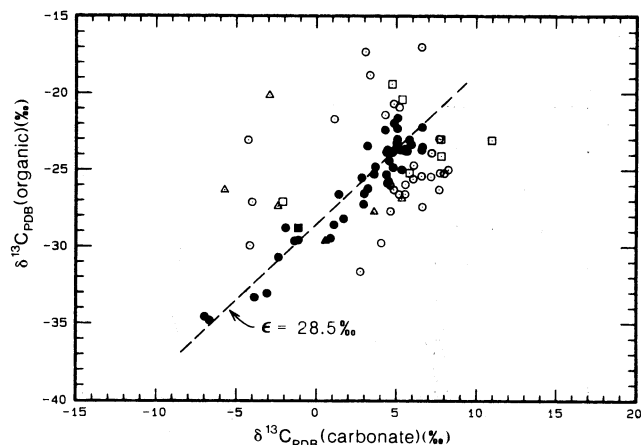


**Fig. 2** Carbon isotopic compositions of samples in which it was possible to analyse both organic and inorganic phases. Squares, samples in which the concentration of organic carbon was  $< 0.2$  mg C per g sample; triangles, samples containing  $< 10\%$  carbonate (as calcite); filled symbols, samples with  $26.5 \leq \epsilon \leq 30.5\%$ .

variations appears in the organic carbon record. We emphasize that our stratigraphic correlation of the three sections was completed independently of the isotopic analyses; thus, the high degree of congruence seen in Fig. 3 demonstrates the potential of chemostratigraphy based on carbon isotopic compositions for accurate intra-basinal correlation of late Proterozoic sedimentary sequences.

The record of isotopic abundances summarized by Fig. 3 encompasses  $> 300$  Myr: the lowermost Cambrian, the Vendian and the Riphean to  $\sim 900$  Myr. Compared with isotopic compositions prevailing during most of the Phanerozoic (and earlier in the Proterozoic, as far as can be determined<sup>30</sup>), its principal features are a general pattern of strong <sup>13</sup>C enrichment during the late Riphean, an extended interval of <sup>13</sup>C depletion in the Vendian and, apparently, several episodes of near-'normal' isotopic compositions in the late Riphean.

As enrichment of <sup>13</sup>C in carbonates is so prominent in the isotopic record summarized in Fig. 3, the process of methanogenic diagenesis should be considered. Fermentative processes yielding methane, often associated with the formation of carbonates enriched in <sup>13</sup>C (ref. 29), apparently have no effect on the isotopic composition of coexisting organic matter. Thus, methanogenic diagenesis shifts points to the right on a graph like that shown in Fig. 2, and it is conceivable that carbonates

**Table 1** Stratigraphy and correlation among sections

East Greenland <sup>13,14</sup>		Northeastern Spitsbergen <sup>7-11</sup>		Nordaustlandet <sup>12</sup>		Tie-points* and chronostratigraphy
Group	Formation	Group	Formation	Group	Formation	
Tillite	Spiral Creek Canyon Tillite Bed 19/20	Oslobreen	{ Kirtonryggen Tokammane Dracoisen	Gotia	{ Klackberget Sveanor Backaberget	-1 540 Myr Cambrian
		Polarisbreen	{ Wilsonbreen Elbobreen Backlundtoppen			0 560 Myr (hiatus) 590 Myr Vendian
		Akademikerbreen	{ Draken Svanbergfjellet Grusdievbreen			3 670 Myr (hiatus) 700 Myr
Eleonore Bay	{ Bed 8 Bed 7	Veteranen	{ Oxfordbreen Glasgowbreen Kingbreen Kortbreen	Roaldtoppen Celsiusberget Franklinsundet	Ryssö Hunnberg Raudstup/Sälodd Norvik Flora Kapp Lord Westmanbukta Persberget	8 800 Myr Upper Riphean
						15 900 Myr

\* Summarizes placement of rock units within chronostratigraphic units and indicates lithostratigraphic tie-points for which ages have been estimated by the authors. Precise placement of tie-points within each section is shown in Fig. 1.

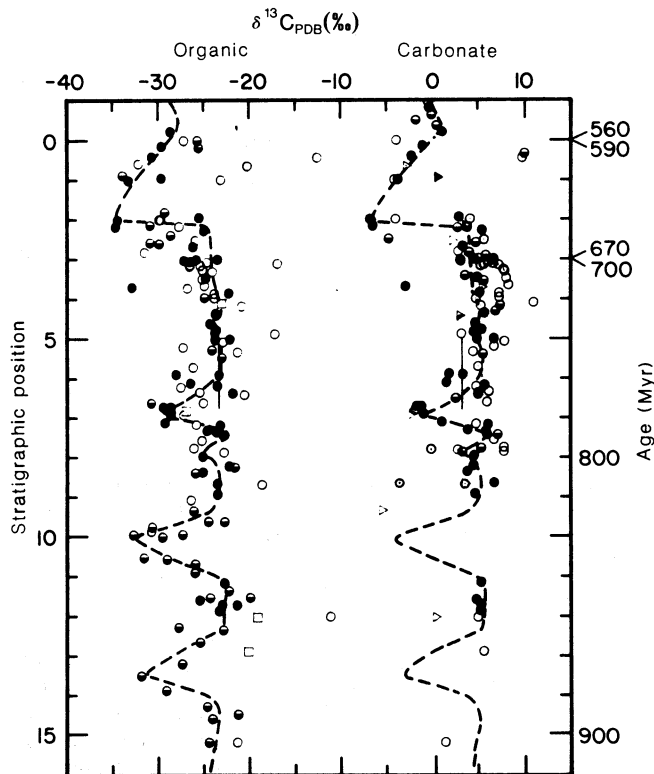


Fig. 3 Isotopic analyses from Fig. 1 pooled and re-plotted on correlated depth scale (numbers at left refer to the tie-points shown in Fig. 1; the scale is thus not linear with respect to either time or thickness of section). Symbols as in Fig. 2 except that half-filled symbols designate samples for which analysis of only one carbon phase (carbonate or organic) was possible. Vertical lines near depth = 6.0 represent a single sample for which stratigraphic placement was uncertain.

represented by some of the open points to the right of the broken line in Fig. 2 have been diagenetically enriched in  $^{13}\text{C}$ . It is, however, extremely unlikely that this process is responsible for the general enrichment of  $^{13}\text{C}$  observed in these sections. To sustain that interpretation, it would be necessary to suggest that, in spite of wide variations in facies (tidal-flat microbial mats, cross-bedded oolites, subtidal dolomitic shales) and carbonate abundance, methanogenesis had, over more than 100 Myr, uniformly affected all of the carbonates that we associate with primary variations in isotopic abundance (filled circles in Fig. 2).

Isotopic compositions within the Vendian Gotia, Polarisbreen and Tillite groups are more variable, reflecting the re-deposition of late Riphean carbonates as detritus<sup>31</sup>, as well as primary variations, but horizons of notably 'light' carbon can be correlated among sections. Cambrian values, obtained only from the Spitsbergen section, range from  $-1.8$  to  $+1.1\%$ , similar to previously published values for Lower Palaeozoic rocks<sup>1</sup>. In Spitsbergen, the base of the Cambrian is recognized by the first appearance of Lontova-type acritarchs and diverse trace fossils of Cambrian aspect; our Lower Cambrian carbonates are associated with *Salterella* and late-*Holmia*-age acritarchs<sup>21</sup>.

**Mechanism and scale of primary variations.** What might account for the enrichment of  $^{13}\text{C}$  in the Upper Riphean sediments of Svalbard and East Greenland? On a basin-wide scale, enrichment of heavy isotopes can be caused by widespread and persistent evaporitic conditions. Isotopically heavy carbonates ( $\delta_c \approx +3.0$ – $5.6\%$ ) are forming today by this mechanism in Shark Bay, Western Australia (J. Ferguson, L. A. Plumb and M. R. Walter, unpublished data), and the heavy carbon in the sections studied here might have a similar origin (although evaporation does not always lead to marked  $^{13}\text{C}$  enrichment; see ref. 32). Two arguments militate against this, however. First, evaporites and

indirect sedimentological evidence of evaporitic environments are conspicuously absent in these sections. Second, a clearly evaporitic sequence from the Proterozoic of northwestern Greenland (the Narssarssuk Formation<sup>33</sup>) has yielded  $0.65 \leq \delta_c \leq 2.65\%$  (mean of 12 samples =  $1.65\%$ ), somewhat heavy relative to early Palaeozoic mean values, but not comparable to the values recorded for Svalbard and East Greenland sediments.

Primary shifts in the isotopic composition of sedimentary carbon can also be due to changes in the isotopic composition of water-column carbonate caused by preferential biological fixation of  $^{12}\text{C}$  into organic material<sup>28,34</sup>. Enhanced rates of burial of organic material lead to greater-than-normal enrichment of  $^{13}\text{C}$  in carbonates<sup>35</sup>.

The scale of these effects can be global or basinal, and assessment of the geochemical significance of isotopic shifts depends strongly on resolution of these alternatives. In a restricted basin, fixation and burial of organic carbon will cause enrichment of  $^{13}\text{C}$  in carbonates if diffusion from the atmosphere and patterns of circulation are unable to maintain isotopic equilibrium with the open ocean. An effect of this kind has been suggested<sup>36</sup> as the explanation for the high levels of  $^{13}\text{C}$  enrichment in the early Proterozoic Lomagundi Group, Zimbabwe. Heavy carbonates might alternatively be due to enrichment of  $^{13}\text{C}$  in carbonate, not in a restricted basin, but throughout the world ocean. An enhancement in the global rate of burial of organic carbon is required to bring about this effect. In the case of the Lomagundi Formation, correlation with coeval sequences from other areas is difficult, so it has not proved possible to resolve the issue by determining whether enrichment was global. Relatively heavy carbon in the Permian, on the other hand, is demonstrably widespread<sup>1,32</sup>.

The possibility that a similar global enrichment occurred in the late Proterozoic can be examined by consideration of all previous reports of carbon-isotopic compositions of middle and late Proterozoic sedimentary carbonates from North America, Africa, India and Australia. Figure 4 shows these data and a summary of carbonate isotopic compositions during the Phanerozoic, together with a curve representative of the isotopic compositions observed in this work. The Phanerozoic and late Proterozoic records differ greatly in temporal resolution, numbers of samples and levels of selectivity. We do not suggest that they can be compared directly in all respects, but contrasts are of such interest that some preliminary consideration is in order.

Comparison (Fig. 4) of the curve representative of isotopic compositions observed in this work with points representing all entries in Table 2 shows that these records are consistent, in that both suggest persistent and significant enrichment of  $^{13}\text{C}$  in late Riphean sedimentary carbonates, as well as episodes of  $^{13}\text{C}$  depletion or normalcy. The scatter of points representative of other rock units around the East Greenland–Svalbard curve is not significant because the stratigraphic positions of many samples are imprecisely defined, and radiometric and biostratigraphic age determinations for many sequences require further work (age uncertainties are estimated in Table 2). Existing data are thus consistent with the idea that the detailed isotopic records observed in this work reflect global trends, but stratigraphic data are insufficient to establish this point in great detail.

**Implications.** It should be evident that isotopic studies can assist in the reconstruction of stratigraphic relationships. Margaritz<sup>37</sup> has shown that systematic variations of the carbon isotopic compositions of sedimentary carbonates can be useful in the correlation of Cretaceous sequences, and Margaritz *et al.*<sup>32</sup> have argued that anomalously heavy carbon can be recognized in Upper Permian sections worldwide. Our study of the Svalbard and East Greenland sections indicates that isotopic chemostratigraphy can facilitate correlations within a basin, and comparison of our data with previously published values suggests that stratigraphic patterns of isotope variations will prove useful in making at least gross correlations between sedimentary basins. Particularly encouraging are comparisons between our data and recently published analyses by Margaritz *et al.*<sup>38</sup> and Tucker<sup>38</sup>

Table 2 Summary of previous analyses of late Proterozoic carbonates

Rock unit*	Age (Myr)†			$\delta_c$	s.d.	n	Ref.
	Min.	Prob.	Max.				
Yakutsk, Siberia, Yudoma Fm	570	575	670	2.2	1.1	6	38
Yakutsk, Siberia, Yudoma Fm	570	585	670	-0.6	1.0	17	38
Nama Group, Schwarzrand Subgroup	570	590	650	-3.1	0.8	7	57
Yakutsk, Siberia, Yudoma Fm	570	595	670	-3.9	0.7	6	38
Nama Group, Kuibis Subgroup I	570	610	650	-0.9	1.3	5	57
Nama Group, Kuibis Subgroup II	570	610	650	2.2	1.2	8	57
Morocco, Serie Lie de Vin	570	610	670	-2.5	1.3	14	39
Adelaide Geosyncline, Marinoan I	570	650	700	7.4	3.6	3	30
Adelaide Geosyncline, Marinoan II	570	650	700	-6.3	2.4	5	30
Adelaide Geosyncline, Nuccaleena Fm	570	650	700	-2.5	0.7	2	58
Kimberley Reg., Late Proterozoic I	570	650	700	-2.9	0.3	5	58
Kimberley Reg., Late Proterozoic II	570	650	700	0.9	1.3	5	58
Amadeus Basin, Pertatataka Fm	625	675	700	5.2	0.5	2	30
Flinders Range, Umberatana Gp	650	675	725	3.3	2.5	3	57
Eleonore Bay Fm, Bed 18	650	700	725	5.2		1	57
S. Norway, Hedmark Gp, Biri Fm	668	700	750	1.7	0.4	11	59
Eleonore Bay Fm, Beds 14-16	700	720	740	5.7	1.0	4	57
Morocco, Dolomite Inferieur	670	735	800	(-2.1	to 6.9)	10	39
Eleonore Bay Fm, Beds 12-13	720	740	760	4.5	0.7	3	57
Adelaide Geosyncline, Sturtian	650	750	750	2.4	0.8	6	30
Adelaide Geosyncline, Tapley Hill Fm	650	750	750	1.8		1	58
Adelaide Geosyncline, Tapley Hill Fm	650	750	750	-3.0	0.6	10	60
Adelaide Geosyncline, Tapley Hill Fm	650	750	750	-0.7	0.4	2	61
Adelaide Geosyncline, Tapley Hill Fm	650	750	750	-0.2	2.3	20	62
Kimberley Region, Landrigan Tillite	650	750	750	-5.5		1	58
Katanga, Lower Kundelungu Series	640	750	840	1.3		1	57
India, Chattisgarh Basin	700	750	850	3.9	1.1	5	57
Eleonore Bay Fm, Bed 9	750	775	800	5.3	0.2	2	57
Taoudenii Syncline, Atar Gp I-11	725	775	825	-0.4		1	57
Kango and Malmesbury Group I	600	775	950	6.6	2.7	4	57
Kango and Malmesbury Group II	600	775	950	-0.3	1.1	11	57
Otavi Gp, Tsumeb Subgroup I	750	780	800	5.1	2.8	6	57
Otavi Gp, Tsumeb Subgroup II	750	780	800	-1.0	0.2	3	57
Taoudenii Syncline, Tifounka Gp, I12	650	800	950	0.7		1	57
Otavi Gp, Upper Abenab Subgroup	750	810	830	2.5	0.0	2	57
Amadeus Basin, Bitter Springs Fm	750	825	900	3.4		1	5
Amadeus Basin, Bitter Springs Fm I	750	825	900	3.5	1.6	8	30
Amadeus Basin, Bitter Springs Fm II	750	825	900	-0.9	2.1	6	30
Taoudenii Syncline, Atar Gp, I-9	725	825	925	0.5	1.9	2	57
Burra Gp, Skillogalee Dolomite	750	850	850	-2.0		1	57
Burra Gp, Skillogalee Dolomite	750	850	850	4.6		1	5
Burra Gp, Skillogalee Dolomite	750	850	850	2.3	1.0	2	‡
Death Valley, Beck Springs Dolomite	800	850	1200	4.2	0.3	13	65
Taoudenni Syncline, Atar Gp, I-7	800	870	900	0.1		1	57
Adelaide Geosyncline, Burra Gp I	840	875	930	-4.5		1	30
Adelaide Geosyncline, Burra Gp II	840	875	930	4.2	0.7	4	30
Katanga, Mwashia Group	840	875	930	-3.5		1	57
Taoudenii Syncline, Atar Gp, I-6	850	880	920	-2.2		1	57
Taoudenii Syncline, Atar Gp, I-5	850	890	925	1.0	0.4	2	57
Katanga, Lower Roan Gp I	930	1,000	1,200	5.7	1.6	2	57
Katanga, Lower Roan Gp II	930	1,000	1,200	-1.1	2.7	11	57
Lake Superior Basin, Sibley Group	1,000	1,050	1,300	-0.3		1	57
Adelaide Geosyncline, Eurelia Beds	1,000	1,060	1,100	3.5	0.8	30	64
Adelaide Geosyncline, Willouran	1,000	1,060	1,100	2.7	1.2	4	30
Glacier National Park, Middle Belt	910	1,075	1,400	0.5		1	65
Oakway Group	850	1,150	1,450	-1.1		1	57
Arizona, Apache Gp, Mescal Limestone	1,150	1,200	1,500	3.1	0.4	16	66
India, Cuddapah Basin	1,100	1,400	1,600	-0.9		1	57
McArthur Basin, HYC (least altered)	1,400	1,640	1,688	-0.3	0.4	7	67
McArthur Basin, McArthur Group	1,590	1,650	1,690	-1.2	1.9	6	30
McArthur Basin, McArthur Gp	1,590	1,650	1,690	-1.0	0.9	6	5
McArthur Basin, Wollgorang Fm	1,590	1,650	1,690	-1.2	1.1	7	§
Birrindudu Basin, Bungle Bungle Dol	1,560	1,650	1,750	-0.7	0.3	7	5

\* Roman numerals appended to rock units designate separate modes of bimodal distributions.

† Minimum, probable and maximum ages estimated by the authors.

‡ I. B. Lambert, unpublished data.

§ M. J. Jackson and T. H. Donnelly, unpublished data.

of sections from Siberia and Morocco, respectively. All three sections show isotopically light intervals in the Vendian, and the Moroccan data, although poorly constrained stratigraphically, show that apparently Upper Riphean beds near the base of the section have highly variable isotopic compositions similar to those assigned to the time interval 645–775 Myr in this work. (Because of this high variability, a point representative of this portion of the Moroccan section is not shown in Fig. 4.) The Moroccan and Siberian rocks also show a short interval of  $^{13}\text{C}$ -enriched carbonate deposition in latest Vendian to earliest Cambrian time, but independent biostratigraphic evidence suggests that rocks of equivalent age are absent in Svalbard and East Greenland<sup>21</sup>. Although inter-basinal resolution may be coarse, any additional means of ascertaining stratigraphic position will be useful for the correlation of Upper Proterozoic sections. The present results also demonstrate that carbon isotopic analyses of organic material can assist in the evaluation of the isotopic record, both in the identification of diagenetic alterations and reconstruction of the record itself.

In addition to their use in stratigraphic correlation, the isotopic data have important implications for phenomena as diverse as palaeoclimatology, end-Proterozoic and early Palaeozoic phosphorite deposition<sup>40</sup>, atmospheric history and biological evolution. Because a global enrichment of  $^{13}\text{C}$  in sedimentary carbonates signals an increase in the rate of burial of organic carbon, it also signals a globally significant shift in oxidation-reduction (redox) processes. Reducing potential flowing to the carbon cycle (in order to allow increased burial of organic carbon, the reduced product in the carbon cycle) must have been diverted from another elemental cycle. The geochemically plausible alternatives are the cycles of sulphur (resulting in an increase in sulphate at the expense of sulphide), iron (resulting in increased precipitation of ferric iron) and oxygen (resulting in accumulation of  $\text{O}_2$ ).

The magnitude of the redox shift can be estimated from the size and duration of the carbon isotopic shift. The flux of carbon in the exogenic cycle in the late Proterozoic is not known. As a point of reference, the present value is  $\sim 2.5 \times 10^{19}$  mol C Myr<sup>-1</sup> (refs 41, 42). In a geochemical carbon cycle characterized by  $\varepsilon = 29\%$  (approximately the value observed in this work), precipitation of carbonates with  $\delta_c = 0\%$  would correspond (at the

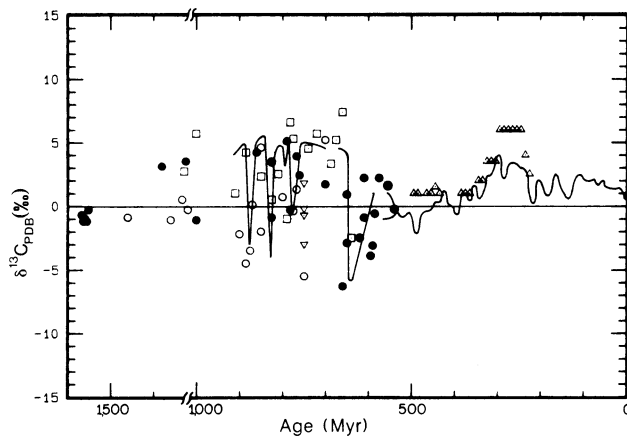


**Fig. 4** Carbon isotopic abundances in carbonates with ages of <1,750 Myr. Note compression of age axis, 1,750–1,000 Myr. The continuous curve in the interval 565–0 Myr is the Phanerozoic carbonate curve compiled by Lindh<sup>68</sup>. Triangles in the same interval represent recent measurements of unaltered portions of brachiopods<sup>69</sup>. The broken curve in the interval 915–540 Myr retraces the carbonate line shown in Fig. 3, with allowance for depositional hiatuses at  $\sim 700$ –670 and  $\sim 590$ –560 Myr. Remaining points represent data summarized in Table 2. Open circles, rock units for which a single isotopic analysis is available; open squares, two to four analyses; filled circles, five or more. Triangles at 750 Myr represent the Tapley Hill Formation, which is possibly non-marine<sup>65</sup>.

modern flux level) to burial of  $4 \times 10^{18}$  mol organic C Myr<sup>-1</sup> (=17% of total flux, assuming  $\delta = 5\%$  for average crustal C). If carbonates instead have  $\delta_c = +5\%$ , the rate of burial of organic carbon is doubled, and oxidized products (sulphate,  $\text{O}_2$ ,  $\text{Fe}^{3+}$ ) must accumulate at a rate equivalent to  $4 \times 10^{18}$  mol  $\text{O}_2$  Myr<sup>-1</sup>. The present atmospheric inventory of  $\text{O}_2$  is  $3.8 \times 10^{19}$  mol. The duration of the late Proterozoic interval of precipitation of carbonates with  $\delta_c = +5\%$  was apparently at least 100 Myr. If the flux of carbon in the exogenic cycle was near modern levels, oxidized material produced during that interval would have been  $\sim 10$  times the present inventory of  $\text{O}_2$ .

The fate of this oxidizing potential is only partly clear. Interpretation of patterns of covariance in the isotopic records of carbon and sulphur suggests that less extreme episodes of oxidation during the Phanerozoic have been largely accommodated by shifts in the redox balance of sulphur<sup>4</sup>. The sulphur isotopic record for the late Proterozoic is far from complete<sup>43</sup>. Until more is known, quantitative estimates of possible shifts in the redox balance of sulphur will be impossible. We note, however, that the flux of sulphur in the exogenic cycle is about 17 times smaller (on a molar basis<sup>31,42</sup>) than that of carbon. Even if all of the sulphur returned to the system by weathering and erosion were initially in the form of pyrite, this flux would be equivalent (at modern levels) to  $3 \times 10^{18}$  mol  $\text{O}_2$  Myr<sup>-1</sup>. In the absence of any other sink for oxidizing potential,  $\text{O}_2$  would thus be expected to accumulate at a rate of at least  $10^{18}$  mol Myr<sup>-1</sup>. The flux of carbon in the exogenic cycle may have been decreased during this interval by 'tectonic tuning'<sup>44</sup>, thus slowing the rate of accumulation of  $\text{O}_2$ , and a significant portion of the excess might have gone into oxidation<sup>45,46</sup> of materials newly exposed at spreading centres<sup>47–49</sup>, but it seems very likely that the period from 700 to 800 Myr ago was a time of important atmospheric oxygen buildup.

It is interesting to speculate as to what factors controlled the timing of this episode of enhanced burial of organic carbon. Probable eukaryotic phytoplankton appear in the record at least 1,400 Myr ago<sup>50</sup>, and must have been well established as important primary producers long before the interval studied here. Morphological changes observed in microfossils from 850–700 Myr ago (ref. 50) might, however, reflect physiological developments which expanded the range of habitable environments by allowing better control of buoyancy or improved interception of nutrients and light. Furthermore, enhanced rates of burial of organic material might be related to tectonic factors. Many of the best known 'Palaeozoic' geosynclinal sedimentary sequences began to accumulate during this interval, including the Iapetus, Adelaiddian and Cordilleran, as well as others in India, China and the Soviet Union<sup>48</sup>. Depositional conditions associated with these developments may well have favoured increased rates of burial of organic carbon<sup>51</sup>. At the same time, conditions of high fertility may have been maintained in the marine environment by more efficient recycling of phosphorus within and just below the photic zone. In the modern global ecosystem, biomineralization and the rapid sinking of faecal pellets both remove phosphate from the surface layers of the ocean and tend to enhance its burial; however, faecal pellets and biosynthetic phosphates appear only later in the geological record. If late Proterozoic organic materials were exclusively microbial and sank more slowly, and if grazing heterotrophs did not package phosphate for rapid sedimentation, more efficient use of phosphate would seem probable.

The end of this era of enhanced burial of organic carbon coincides with the major Eocambrian glaciation. The periodic returns to 'normal' carbon isotopic compositions within the era may coincide with earlier glaciations<sup>48</sup>. The occurrence of major glaciations implies the existence of a strong climatic gradient which, in turn, is very likely to have affected circulation within the ocean, possibly encouraging the development of deep circulation and reducing rates of burial of organic material. By the close of the Varangian glaciation, evolutionary developments had occurred which countered the factors described above, and

very high rates of burial of organic carbon were not re-established. It is also possible, of course, that O<sub>2</sub> pressures equal to or higher than present levels were attained and acted to prevent burial of organic material by establishing a particularly aggressive environment.

An increase in atmospheric O<sub>2</sub> levels 700–800 Myr ago is of great palaeobiological interest because many authors have argued that the time of appearance of macroscopic metazoans was constrained by oxygen tensions sufficient to permit epithelial diffusion of oxygen across multiple cell layers, support metazoan exercise metabolism, and permit collagen synthesis (see, for example, refs 52–56). Until now, there have been no geochemical data to support this idea; however, as the conspicuous fossil record of animals begins just after the interval of heavy carbon deposition, it may be that the late Proterozoic isotopic record is supplying the evidence needed to support this concept. Additional data are required to evaluate this possibility. Detailed

secular curves for organic and carbonate carbon need to be established for other Upper Proterozoic sections, and these must be complemented by similar curves for sulphur. It is clear, however, that the carbon isotopic record will be an important part of the evidence on which reconstruction of late Proterozoic evolution, environmental history, and their interaction through the carbon cycle will eventually be based.

We thank the Commission on Scientific Research in Greenland and the Governor of Svalbard for permission to work in national park areas. The Nordaustlandet samples were collected by A.H.K. as a member of the Cambridge Svalbard Expedition (W. B. Harland, director). We thank H. D. Holland, W. T. Holser and J. C. G. Walker for discussions. Research was supported in part by grants from the NSF (A.H.K., K.S.) and NASA (NGR 15-003-118 to J.M.H.). I.B.L. acknowledges support for the Baas Becking Laboratory from BMR, CSIRO and AMIRA.

Received 19 December 1985; accepted 7 May 1986.

1. Holser, W. T. in *Patterns of Change in Earth Evolution* (eds Holland, H. D. & Trendall, A. F.) 123–143 (Springer, Berlin, 1984).
2. Shackleton, N. J., Hall, M. A., Line, J. & Chang Shuxi *Nature* **306**, 319–322 (1983).
3. Arthur, M. A. in *Climate in Earth History* (eds Berger, W. H. & Crowley, J. C.) 55–67 (National Academy Press, Washington, 1982).
4. Veizer, J., Holser, W. T. & Wilgus, C. K. *Geochim. cosmochim. Acta* **44**, 579–587 (1980).
5. Schidlowski, M., Hayes, J. M. & Kaplan, I. R. in *Earth's Earliest Biosphere* (ed. Schopf, J. W.) 149–185 (Princeton University Press, 1983).
6. Kulling, O. *Geogr. Annl.* **16**, 161–254 (1934).
7. Wilson, C. B. *Geol. Mag.* **45**, 305–327 (1958).
8. Wilson, C. B. *Geol. Mag.* **48**, 89–116 (1961).
9. Wilson, C. B. & Harland, W. G. *Geol. Mag.* **101**, 198–219 (1964).
10. Hambrey, M. J. *Geol. Mag.* **119**, 527–642 (1982).
11. Swett, K. *Geol. Mag.* **118**, 225–336 (1981).
12. Flood, B., Gee, D. G., Hjelte, A., Siggerud, T. & Winsnes, T. S. *Norsk Polarinst. Skr.* **146**, 1–139 (1969).
13. Haller, J. *Geology of the East Greenland Caledonides* (Wiley, New York, 1971).
14. Eha, S. *Meddr Grønland* **11**, 1–1095 (1953).
15. Vidal, G. *Grøn. Geol. Unders. Bull.* **134**, 1–40 (1979).
16. Knoll, A. H. *Geol. Mag.* **119**, 269–279 (1982).
17. Knoll, A. H. & Swett, K. *Palaentology* **28**, 451–473 (1985).
18. Raaben, M. Ye & Zabrodin, Y. Ye. *Dokl. Akad. Nauk SSSR* **184**, 676–679 (1968).
19. Swett, K. & Knoll, A. H. *J. sedim. Petrol.* (in the press).
20. Downie, C. *Trans. R. Soc. Edinburgh* **72**, 257–285 (1982).
21. Knoll, A. H. & Swett, K. *J. Paleont.* (in the press).
22. Harland, W. G. & Gayer, R. A. *Geol. Mag.* **109**, 289–314 (1972).
23. Roberts, D. & Gale, G. H. in *Evolution of the Earth's Crust* (ed. Tarling, D. H.) 255–342 (Academic, London, 1978).
24. Wedeking, K. W., Hayes, J. M. & Matzigkeit, U. in *Earth's Earliest Biosphere* (ed. Schopf, J. W.) 428–442 (Princeton University Press, 1983).
25. Wachter, E. A. & Hayes, J. M. *Chem. Geol.* **52**, 365–374 (1985).
26. Santrock, J., Studley, S. A. & Hayes, J. M. *Analyt. Chem.* **57**, 1444–1448 (1985).
27. Brand, U. & Veizer, J. *J. sedim. Petrol.* **51**, 987–997 (1981).
28. Hayes, J. M. in *Earth's Earliest Biosphere* (ed. Schopf, J. W.) 291–301 (Princeton University Press, 1983).
29. Irwin, H., Curtis, C. & Coleman, N. *Nature* **269**, 209–213 (1977).
30. Veizer, J. & Hoefs, J. *Geochim. cosmochim. Acta* **40**, 1387–1395 (1976).
31. Fairchild, I. J. *Nature* **304**, 714–716 (1983).
32. Margaritz, M., Anderson, R. Y., Holser, W. T., Saltsman, E. S. & Garber, J. *Earth planet. Sci. Lett.* **66**, 111–124 (1983).
33. Strother, P. K., Knoll, A. H. & Barghoorn, E. S. *Palaentology* **26**, 1–32 (1983).
34. Broecker, W. S. *J. geophys. Res.* **75**, 3553–3557 (1970).
35. Scholle, P. A. & Arthur, M. A. *Bull. Am. Ass. Petrol. Geol.* **64**, 67–87 (1980).
36. Schidlowski, M., Eichmann, R. & Junge, C. E. *Geochim. cosmochim. Acta* **40**, 449–455 (1976).
37. Margaritz, M. *Sedim. Geol.* **45**, 115–123 (1985).
38. Margaritz, M., Holser, W. T. & Kirschvink, J. L. *Nature* **320**, 258–259 (1986).
39. Tucker, M. E. *Nature* **319**, 48–50 (1986).
40. Cook, P. J. & Shergold, J. H. *Nature* **308**, 231–236 (1984).
41. Lasaga, A. C., Berner, R. A. & Garrels, R. M. in *The Carbon Cycle and Atmospheric CO<sub>2</sub>: Natural Variations Archean to Present* (eds Sundquist, E. T. & Broecker, W. S.) 397–411 (American Geophysical Union, Washington, 1985).
42. Arthur, M. A., Dean, W. E. & Schlanger, S. O. in *The Carbon Cycle and Atmospheric CO<sub>2</sub>: Natural Variations Archean to Present* (eds Sundquist, E. T. & Broecker, W. S.) 504–529 (American Geophysical Union, Washington, 1985).
43. Claypool, G. E., Holser, W. T., Kaplan, I. R., Sakai, H. & Zak, I. *Chem. Geol.* **28**, 199–260 (1980).
44. Worsley, T. R., Moody, J. B. & Nance, R. D. in *The Carbon Cycle and Atmospheric CO<sub>2</sub>: Natural Variations Archean to Present* (eds Sundquist, E. T. & Broecker, W. S.) 561–572 (American Geophysical Union, Washington, 1985).
45. McDuff, R. E. & Edmond, J. M. *Earth planet. Sci. Lett.* **57**, 117–132 (1982).
46. Walker, J. C. G. *Mar. Chem.* (in the press).
47. Veizer, J., Compston, W., Clauer, N. & Schidlowski, N. *Geochim. cosmochim. Acta* **47**, 295–302 (1983).
48. Windley, B. F. *The Evolving Continents* (Wiley, London, 1977).
49. Bond, G. C., Nickerson, P. A. & Kominz, M. A. *Earth planet. Sci. Lett.* **70**, 325–345 (1984).
50. Vidal, G. & Knoll, A. H. *Mem. geol. Soc. Am.* **161**, 265–277 (1983).
51. Walter, M. R. *Baas Becking Geobiol. Lab. A. Rep.*, 45–56 (1982).
52. Raff, R. A. & Raff, E. C. *Nature* **228**, 1003–1005b (1970).
53. Runnegar, B. *J. geol. Soc. Aust.* **29**, 395–411 (1982).
54. Runnegar, B. *Alcheringa* **6**, 223–239 (1982).
55. Cloud, P. *Paleobiology* **2**, 351–387 (1976).
56. Towe, K. M. *Proc. natn. Acad. Sci. U.S.A.* **65**, 781–788 (1970).
57. Schidlowski, M., Eichmann, R. & Junge, C. E. *Precamb. Res.* **2**, 1–69 (1975).
58. Williams, G. E. *J. geol. Soc. Aust.* **26**, 377–386 (1979).
59. Tucker, M. E. *Precamb. Res.* **22**, 293–315 (1983).
60. Lambert, I. B., Knutson, J., Donnelly, T. H., Etminan, H. & Mason, M. *Miner. Deposita* **19**, 266–273 (1984).
61. Knutson, J., Donnelly, T. H. & Tonkin, D. G. *Econ. Geol.* **78**, 250–274 (1983).
62. Lambert, I. B., Donnelly, T. H. & Rowlands, M. J. *Miner. Deposita* **15**, 1–18 (1980).
63. Tucker, M. E. *Geology* **10**, 7–12 (1982).
64. Lambert, I. B., Donnelly, T. H., Etminan, H. & Rowlands, N. J. *Econ. Geol.* **79**, 461–475 (1984).
65. Hoering, T. C. *Yb. Carnegie Instn. Wash.* **61**, 190–191 (1962).
66. Beeunas, M. A. & Knauth, L. P. *Geol. Soc. Am. Bull.* **96**, 737–745 (1985).
67. Rye, D. & Williams, N. E. *Econ. Geol.* **76**, 1–26 (1981).
68. Lindh, T. B. thesis, Univ. Miami (1983).
69. Popp, B. N., Anderson, T. F. & Sandberg, P. A. *Geol. Soc. Am. Bull.* (in the press).